Investigation of parametters in Oscillations of Newton's Cradle

Amirmehdi Jafari Fesharaki
Sharif University of Technology, Ariaian Young Innovative Minds Institute, AYIMI, Tehran, Iran, http://www.ayimi.org.

E-mail: amiroo23jf@gmail.com

(Received 8 October 2019, accepted 24 December 2019)

Abstract

This is a problem related to oscillations of a Newton's cradle which will gradually decay until the spheres come to the rest. The effect of several parameters such as number, material and alignment of the spheres on the rate of decay in this research have been investigated. The collision between two balls was our initial observation and then it was extended to a higher number of balls. A comparison between middle and side ball and the effect of number of the releasing balls and alignment are investigated theoretically which shows the decay in collisions and also increasing the number of the balls will cause increasing the rate of decay too. It also shows that as we use more elastic materials, the rate of decay decreases in our experiment.

Keywords: Oscillation, Newton's cradle, Collision, Elastic Materials.

Resumen

Este es un problema relacionado con las oscilaciones de la cuna de Newton, que decaerá gradualmente hasta que las esferas lleguen al resto. Se ha investigado el efecto de varios parámetros como el número, el material y la alineación de las esferas sobre la tasa de descomposición en esta investigación. La colisión entre dos bolas fue nuestra observación inicial y luego se extendió a un mayor número de bolas. Se investiga teóricamente una comparación entre la bola media y lateral y el efecto del número de las bolas de liberación y la alineación, que muestra la descomposición en colisiones y también el aumento del número de bolas causará un aumento de la velocidad de descomposición. También muestra que a medida que usamos más materiales elásticos, la tasa de descomposición disminuye en nuestro experimento.

Palabras clave: Oscilación, cuna de Newton, colisión, materiales elásticos.

PACS: 01.30.Os, 01.40.–d, 01.50.–i **ISSN 1870-9095**

I. INTRODUCTION

Newton's cradle is constructed from a series of pendulums (usually five in number) abutting one another. Each pendulum is attached to a frame by two strings of equal length angled away from each other. If these strings were not same in length, the balls would then be unbalanced. This string arrangement restricts the pendulums' movements to the same plane. In Newton's cradle when the first ball is released, it hits the second ball then transfers its momentum and energy to the last ball through the middle balls. This process repeats in reverse until the spheres come to the rest and all of the energy is dissipated. The behavior of the pendulum follows from the conservation of momentum and kinetic energy only in the case of two pendulums (Fig.1) [1].

The phenomenon causes swinging pendulums to synchronize when they are close together, but if we have a number of pendulums, there are unknown parameters to be calculated from the initial conditions.

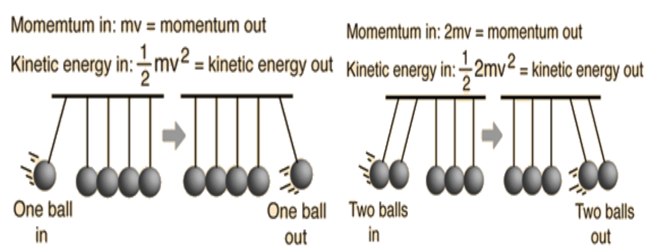

FIGURE 1. Demonstration of conservation of momentum and conservation of energy in Newton's cradle [2].

When a ball on one end of the cradle is pulled away from the others and then released, it strikes the next ball in the cradle, which remains motionless. But the ball on the opposite end of the row is thrown into the air, then swings back to strike the other balls, starting the chain reaction again in reverse (Fig.2).

II. MATERAIALS, DEVICES AND METHOD

A. Materaials and devices

When a ball on one end of the cradle is pulled away from the others and then released, it strikes the next ball in the cradle, which remains motionless. But the ball on the opposite end of the row is thrown into the air, then swings back to strike the other balls, starting the chain reaction again in reverse (Fig.2).

Two cradles in different materials, steel and copper, with 2 up to 5 number of balls, are used in this experiment.

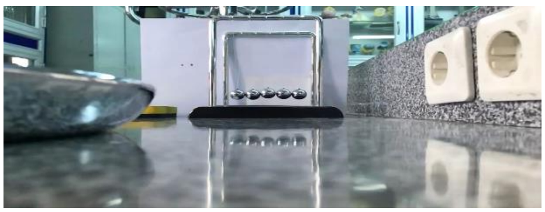

FIGURE 2. A Newton's Cradle setup.

B. Methods and modeling

This is started with modeling the collisions between two balls in the perfectly elastic condition. For perfectly elastic collision between two spheres, elasticity and ratio between two spheres' masses is equal to 1. When the first ball hits the second ball, all of its momentum and energy is transferred to the next ball and it starts moving with the first ball's initial velocity. When the first ball collides with the second, the first ball stops, and its momentum is transferred to the second ball until it reaches the last ball. In perfectly elastic collision between two balls, we have (Eq. 1) (Fig.3 a and b):

$$\left.\begin{aligned} \varepsilon\frac{m_1v^2}{2} &= \frac{m_1{v_1}^2}{2}+\frac{m_2{v_2}^2}{2} \\ m_1v &= m_1v_1+m_2v_2 \end{aligned}\right\} \xrightarrow{\alpha=\frac{m_2}{m_1},\ \varepsilon=1} \left\{\begin{aligned} v_1 &= 0 \\ v_2 &= v \end{aligned}\right. \quad (1)$$

(a) (b)

FIGURE 3. Perfectly elastic collision**;** a) Before collision, b) After collision.

Now the collision is expanded to higher number of balls in the ideal condition (Fig. 4 a and b). For higher number of balls, when the first ball hits the others, its momentum and energy is transferred to the last ball which means that the middle balls do not gain any energy and they only transfer the energy from first to the last ball.

(a) (b)

FIGURE 4. Collisions of a higher number of balls; a) Before collision, b) After collision.

The experiment with five billiard balls shows the energy and momentum is transferred from the first to the last ball, which the middle balls have a slight movement (Fig.5). The reason is that the collisions are not perfectly elastic and there is a dissipation of energy in the whole system, which means we need to improve our theory.

FIGURE 5. Collisions of billiard balls.

For improving the theory of collisions, we modeled the collision between two spheres with springs and dashpots [3], where **k** is the spring constant and **γ** is the dissipation constant. In this model, springs are for the elastic part of a collision and dashpots are for the dissipative part (Fig. 6). Forces are applied to the spheres in each collision are gravitational force, air drag force, and the elastic force.

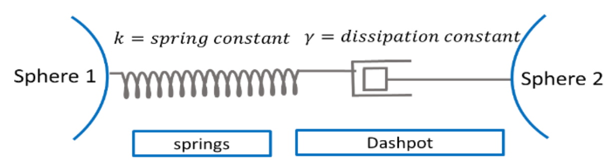

FIGURE 6. Modeling the collision between two spheres.

III. THEORY

A. Forces applying in each collision

The force could be divided in two parts; dissipative and elastic forces. The elastic part is modeled using springs and the dissipative part, which in dashpots as shown in figure (5).

A.1 Elastic force

Before calculating the force in collision between two spheres, a simple example for compression between two cylinders is explained. For compression between two cylinders, due to the stress-strain relation, where E is the young modulus, S the effective area and Δl as the length of cylinders' compression, force could be obtained (Eq. 2) (Fig. 7 a and b). The point is that in compression between two cylinders, the effective area is constant in the whole collision; however, for two spheres this would change.

$$E\,\frac{\Delta l}{l}=\frac{F}{s}. \quad (2)$$

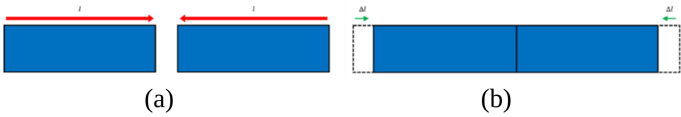

FIGURE 7. Compression between two cylinders; a) Before compression, b) After compression.

In compression between two spheres, the effective area is increasing by the time. When the pressure is zero, they only have a contact point (Fig. 8a) but as this pressure is increased, this contact point transforms to a contact area (Fig. 8b).

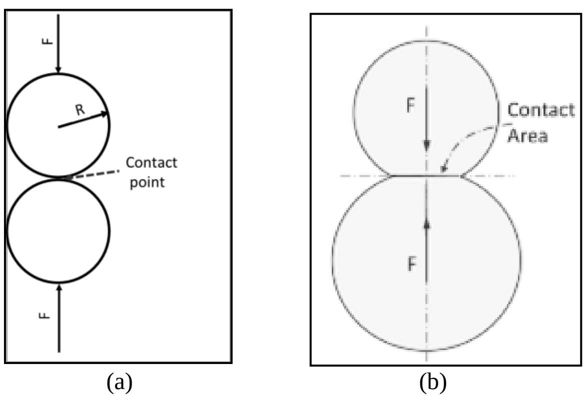

FIGURE 8. Compression of two spheres; a) Contact point (No pressure), b) Contact area (with pressure).

Due to the stress-strain relation, force depends on the effective area; it means that as the effective area is increased, the force between spheres increases but this force is not a linear function of the length of compression anymore. Due to the Hertzian theory [1], the force could be obtained using this equation where α is a power equal to 3/2 and ξ is the length of compression (Eq. 3) (Fig.9). K is the spring constant and could be obtained using (Eq. 4) where E is the young modulus and ν is the Poisson ratio.

$$F = k\,\xi^{\alpha}, \tag{3}$$

$$k = \frac{E\sqrt{2r}}{3(1-\nu^2)} \;. \tag{4}$$

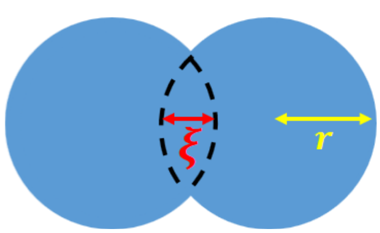

FIGURE 9. Compression between two spheres.

A.2 Viscoelastic dissipation force

Next, we have the dissipation force which was mentioned before as dashpots. The viscoelastic dissipation force for cylinders could be obtained using (Eq. 5) (Fig. 10a), although this force for two spheres could be obtained using this equation due to the hertz-kuwabara-kono, which again has a power of 3/2 on the length of compression (Eq. 6) (Fig. 10b).

$$F_{diss} = -\gamma' \frac{d}{dt}(\xi), \tag{5}$$

$$F_{diss} = -\gamma \frac{d}{dt}(\xi^{\frac{3}{2}}). \tag{6}$$

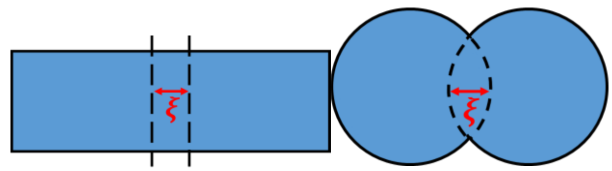

FIGURE 10. The viscoelastic dissipation force; a) Compression of two cylinders, b) Compression of two spheres.

B. The gravitational force acting on a ball

The next force that is acting on each ball is gravitational force (Fig. 11). The gravitational force is calculated in first approximation of x/l. In this approximation, sin (Θ) would be equal to x/l and cos (Θ) could be considered as one. Due to Newton's second law, we have these two equations in directions of x-axis and direction of the string. In first approximation, T=mg and the gravitation force in x-axis could be obtained using (Eq. 9).

$$T - mg\cos(\theta) = \frac{m(\dot{x}^2 + \dot{y}^2)}{l}, \tag{7}$$

$$m\ddot{x} = -T\sin(\theta), \tag{8}$$

$$F_g = -\frac{mgx}{l}. \tag{9}$$

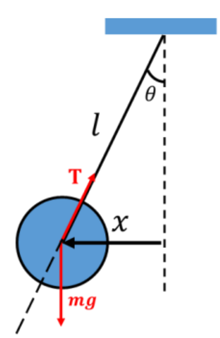

FIGURE 11. The gravitational force acting on a ball.

C. The air drag force acting on a ball

The final force which is acting on a ball is the air drag force. This force could be obtained using (Eq. 10) due to the Stocks' law, where R is the radius of the sphere and μ is the dynamic viscosity of air (Fig. 12).

$$F = 6\pi\mu R v \ . \qquad (10)$$

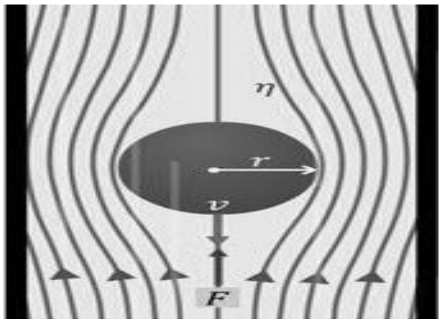

FIGURE 12. The air drag forcé.

D. The equation of motion for n th sphere

Finally, we can write the equation of motion using the four equations which was mentioned before. The equation of motion for the n-th sphere could be obtained using (Eq. 11) (Fig. 13).

$$m\ddot{x}_n = k\xi_{n,n-1}^{\frac{3}{2}} + \gamma\frac{d}{dt}\left(\xi_{n,n-1}{}^{\frac{3}{2}}\right)$$

$$-k\xi_{n+1,n}^{\frac{3}{2}} - \gamma\frac{d}{dt}\left(\xi_{n+1,n}{}^{\frac{3}{2}}\right)$$

$$-\eta\dot{x}_n - \frac{mg(x_n - x_{0,n})}{l}. \qquad (11)$$

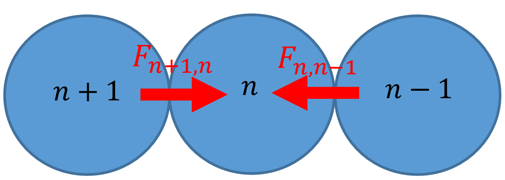

FIGURE 13. Force acting in each collision to the *n*-th sphere.

By expanding this equation, we reach the final equation (Eq. 12) (Fig. 14).

$$m\ddot{x}_n = k((2R - |x_n - x_{n-1}|)^{\frac{3}{2}} -$$

$$(2R - |x_{n+1} - x_n|)^{\frac{3}{2}}) -$$

$$\eta\dot{x}_n - \frac{mg(x_n - (n-1)*2R)}{l} +$$

$$\gamma\frac{d}{dt}((2R - |x_n - x_{n-1}|)^{\frac{3}{2}} -$$

$$(2R - |x_{n+1} - x_n|)^{\frac{3}{2}}) \ . \qquad (12)$$

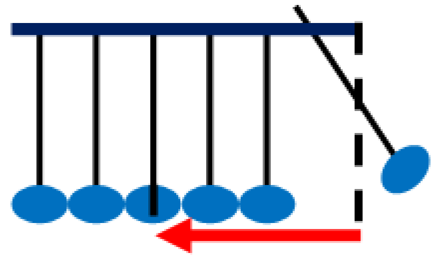

FIGURE 14. Motion for n-th sphere.

IV. COMPARISON OF THEORY AND EXPERIMENT

The blue trend shows the experimental results for the angle versus time for 5 steel balls (Fig. 15a). The red trend in this figure is the theoretical fit by solving (Eq. 12) using numerical approach (Fig. 15b). In solving this equation, the only fitting parameter is γ.

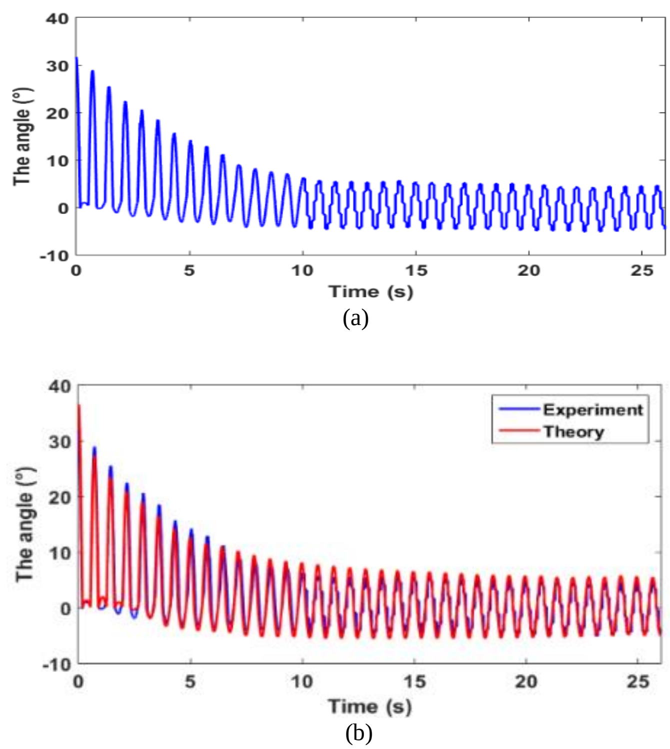

FIGURE 15. Comparison of theory and experiment; a) Experimental results, b) Theoretical fit.

But a more comparable parameter is needed for comparing the rate of decay. As it is shown, an exponential function can be fitted to the maximum angle of each period (Fig. 16). In this function, θ_0 is the initial angle and α is the only fitting parameter which is defined as the parameter of decay (Eq. 13). The increase in α shows that the rate of decay is increasing.

$$\theta_{max} = \theta_0 e^{-\alpha t} \ . \qquad (13)$$

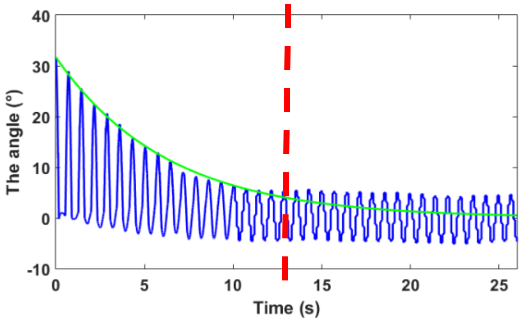

FIGURE 16. Exponential function fitting the maximum angle in each period.

This exponential function is completely fitting up to a certain point, but after that the exponential function and the experimental results do not fit anymore (Fig. 15). Therefore, the whole movement is divided into two phases. The first phase is when all of the spheres have collision and their amplitude is not equal but after a point, the second phase starts. In this phase there is no collision between the spheres and they oscillate with a same amplitude (Fig. 17 a and b). This means that in the first phase because of the collisions, there is a higher amount of energy loss than the second phase.

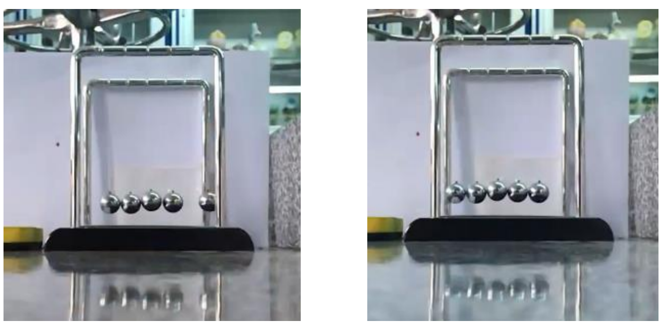

(a) (b)

FIGURE 17. Different phases of movement; a) First phase (with collision)**,** b) Second phase (without collision).

A. The effect of number of balls

By increasing the number of the balls, *α*, the parameter of decay increases which means that the rate of decay increases. The comparison of exponential fits, for different number of steel balls is studied. As the number of balls increases, the time of decay decreases and the energy is dissipated faster.

When the number of the spheres is increased, the number of collisions also increases; in each collision there is a certain amount of energy loss which means, as the number of balls increases the dissipation of energy increases, this concludes in increasing the rate of decay (Fig. 18).

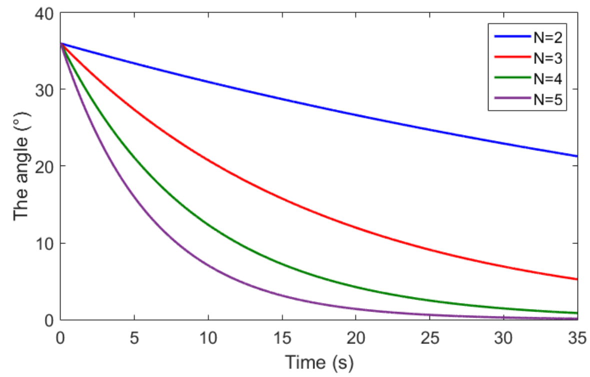

FIGURE 18. Angle versus time for different numbers of spheres.

Here, there is a figure, which shows the relation between α, the parameter of decay, and the number of spheres. The interesting point is that the parameter of decay is a linear function of the number of the balls (Fig. 19).

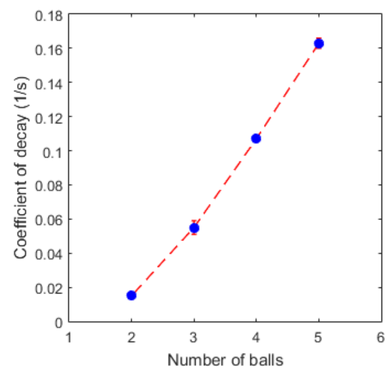

FIGURE 19. Coefficient of decay (α) versus the number of spheres.

B. The effect of the materials

Next, we have the effect of different materials on the rate of decay. We experimented with two different materials, copper and steel (Fig. 20). For two spheres, copper has a higher rate of decay than steel; however, while the number of balls is increased, the copper's rate of decay remains higher than steel. The reason is that copper has a lower elasticity in comparison with steel. It means that in each collision copper has more dissipation of energy which increases the rate of decay (Fig. 21).

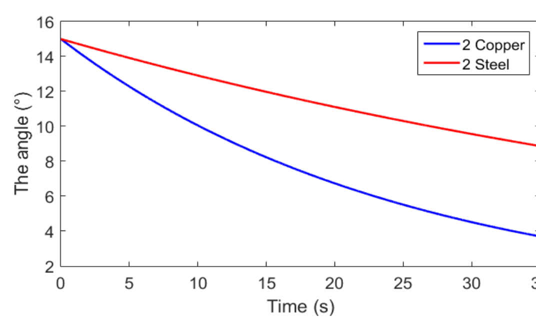

FIGURE 20. Comparison of 2 steel and copper spheres.

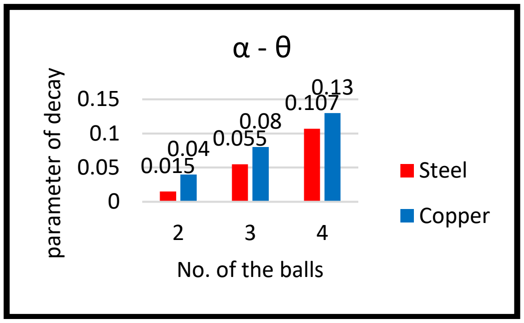

FIGURE 21. The effect of material on the rate of decay.

C. The effect of the initial angle

The coefficient of decay in different initial angles is compared to find the relation between this the initial angle and the Newton's cradle movement (Fig. 22). It was experimented in different number of spheres to have a stronger justification. As shown, changing the initial angle does not change the coefficient of decay which completely agrees with the theory which was mentioned before (Eq. 13).

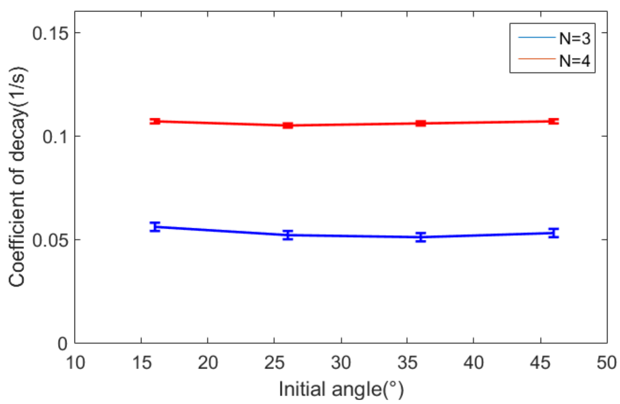

FIGURE 22. The relation between coefficient of decay (α) and initial releasing angle.

D. THE COMPARISON OF THE MIDDLE AND SIDE BALLS

In figure (Fig. 23) the middle ball and the side ball movements are compared. For the side balls, as the time passes, the amplitude of each oscillation decreases; however, this amplitude in middle balls increases. It shows that side balls transfer a part of their momentum and energy to the middle balls until they all fluctuate with a same amplitude, the second phase which was mentioned before starts here. At this point they will not have any collisions and the only dissipation force is the air drag force.

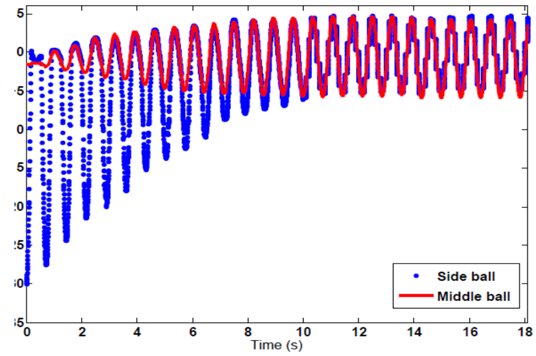

FIGURE 23. The comparison between middle ball and the side ball.

E. The number of releasing spheres

The next experiment was the effect of the number of initial releasing spheres on the rate of decay, while the ratio of the number of releasing spheres to the number of total spheres stayed constant (Fig. 24). The results show, as the number of releasing spheres is increased, the rate of decay increases. The reason is that when two spheres are released instead of one, they will have collisions together which dissipates higher energy.

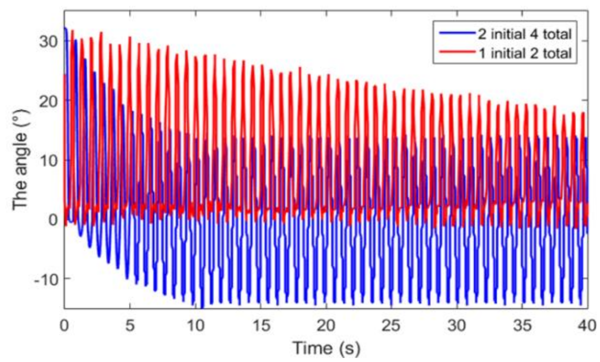

FIGURE 24. Effect of changing the number of releasing spheres.

F. THE ALIGNMENT OF THE SPHERES

If the line, which connects the center of the spheres, has an angle of (Θ) with horizontal axis, the force between balls would have a component in other directions in addition of x-axis; it means that the force in x-axis is equal to $F\cos(\Theta)$ (Fig. 25).

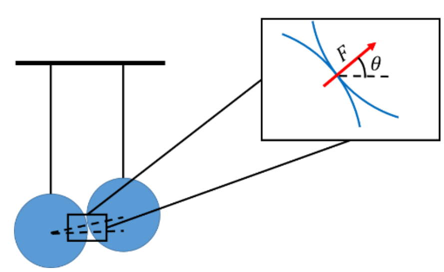

FIGURE 25. The alignment of spheres.

There is a comparison for an aligned and out of align cradle below which shows a slight change in the results (Fig. 26).

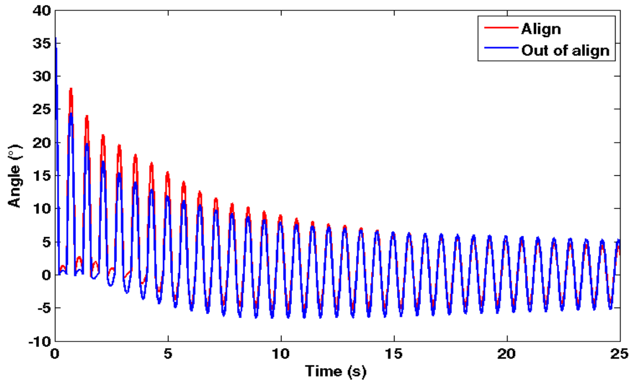

FIGURE 26. Results of changing the alignment.

V. CONCLUSIONS

In this research, first the collision between two balls was investigated in perfectly elastic collisions and then it was expanded to a higher number of balls. The results showed that it does not have an agreement with the real life experiments. Then the theory was improved and this collision was modeled with springs and dashpots using hertzian theory for elastic part and hert-kuwabara-kono theory for dissipation part of the force. Using this method an improved equation of motion was written for each sphere in the cradle and solved numerically.

This improvement made a perfect agreement between theory and experiments; however, a comparable parameter was needed for comparing the rate of decay by changing different parameters. For this reason, an exponential function was fitted to the maximum angle of each period (Eq. 13). Then (α) was defined as coefficient of decay due to (Eq. 13). Next, the whole movement was divided into two different phases due to their behavior in these phases. In the first phase, spheres have collision and fluctuate with different amplitudes, but in the second phase they start fluctuating together without any collision.

The effect of different parameters, such as number, material, initial releasing angle and the alignment of the spheres on the rate of decay are studied too. As the number of the spheres is increased, the rate of decay increases too but by changing the initial releasing angle, the coefficient of decay does not change. It is found that using more elastic materials causes a lower rate of decay. Different alignment results in some slight changes in the movement of the cradle. After changing these parameters, we also had a comparison between middle and side spheres. The final study was changing the number of releasing spheres while the number of releasing spheres to the number of total spheres was constant. This showed that as the number of releasing spheres was increased, the rate of decay increase too.

ACKNOWLEDGEMENTS

This research is one of the IYPT 2019 problems which Team Iran participates in this great international physics tournament every year. I would like to thank Dr. Hossein Salari as the supervisor and AYIMI institute which is the organizer of several scientific activities and competitions. Iran national team is selected by PYPT (Persian Young Physicists' Tournament, AYIMI) to challenge with other teams from several countries in IYPT.

REFERENCES

[1] Palermo, E., *How Does Newton's Cradle Work?*, (2013), https://www.livescience.com/39271-how-does-newtons-cradle-work.html.

[2] http://hyperphysics.phy-astr.gsu.edu/hbase/elacol.html

[3] Dashpots, (2017). https://abaqus-docs.mit.edu/2017/English/SIMACAEELMRefMap/simaelm-c-dashpot.htm#hj-top